

Decentralized Optimal Scheduling for Charging and Discharging of Plug-In Electric Vehicles in Smart Grids

Hao Xing, *Student Member, IEEE*, Minyue Fu, *Fellow, IEEE*, Zhiyun Lin, *Senior Member, IEEE*, and Yuting Mou

Abstract—This paper focuses on the procurement of load shifting service by optimally scheduling the charging and discharging of PEVs in a decentralized fashion. We assume that the energy flow between PEVs and the grid is bidirectional, i.e., PEVs can also release energy back into the grid as distributed generation, which is known as vehicle-to-grid (V2G). The optimal scheduling problem is then formulated as a mixed discrete programming (MDP) problem, which is NP-hard and extremely difficult to solve directly. To get over this difficulty, we propose a solvable approximation of the MDP problem by exploiting the shape feature of the base demand curve during the night, and develop a decentralized algorithm based on iterative water-filling. Our algorithm is decentralized in the sense that the PEVs compute locally and communicate with an aggregator. The advantages of our algorithm include reduction in computational burden and privacy preserving. Simulation results are given to show the performance of our algorithm.

Index Terms—Decentralized control, load shifting, optimal scheduling, plug-in electric vehicle, smart grid, vehicle-to-grid.

I. INTRODUCTION

THE excessive emission of greenhouse gases and the decreasing petroleum energy have raised a big concern for years. It is generally accepted that plug-in electric vehicles (PEVs) are one of the solutions [1]. Besides the environmental benefits, electricity is cheaper than petroleum fuels, which rids a nation of the dependence on imported oil. PEVs will also increase the energy efficiency [2]. However, the introduction of PEVs will have a significant impact on the distribution system. The uncoordinated charging of PEVs may lead to a new peak load or worsen the current peak load, and may consequently

cause serious damage to the distribution system and other electrical appliances [3]. On the other hand, if properly scheduled, PEVs can be utilized for the provision of ancillary services, which is also known as demand side management (DSM). The development of smart chargers, advanced metering infrastructures (AMIs), and communication systems enable us to develop appropriate algorithms for the DSM using PEVs [4].

Massive efforts have been made to explore PEVs' potential for DSM. According to the direction of energy flow between PEVs and grids, existing works can be classified into two categories: those utilizing the charging process only, also known as grid-to-vehicle (G2V), and those considering both G2V and V2G. References [5]–[10] consider G2V only and propose different algorithms to the charging scheduling of PEVs. In [5], the authors formulate the charging problem as a class of finite-horizon dynamic games, and propose a decentralized method. Reference [6] presents a comprehensive analysis of the load shifting problem via PEVs, and proposes an optimal decentralized charging (ODC) algorithm. References [7]–[9] present a portfolio of decentralized algorithms, which are all based on a decentralized water-filling-based algorithm, to flatten the load curve of low-voltage transformers and achieve the optimal charging scheduling. Network-controlled PEVs are used for the regulation of supply grid in California with renewable energy of different penetration rates in [10]. Smart inverters for V2G enable the PEVs to release power back to the grid, which enable researchers to utilize both G2V and V2G [11]. Reference [12] aims at the minimization of aggregated charging cost of PEVs and proposes decentralized algorithms for globally and locally optimal scheduling, respectively, which can effectively deal with the random arrivals of PEVs. In [13], using dynamic programming, the authors find an optimal charging and discharging scheduling algorithm under uncertainty in a smart grid with renewable energy sources. In [14], a stochastic security-constrained unit commitment (Stochastic SCUC) model is used to minimize the expected grid operation cost while considering the random behavior of the PEVs. Reference [15] studies the load regulation of a single household using PEVs such that the aggregated demand of the entire network is regulated. An optimal centralized scheduling method to jointly control the electricity consumption of home appliances and PEVs is proposed in [16] to increase the reliability and stability of microgrids.

Since smart grids are large-scale systems, where centralized algorithms may fail due to lack of scalability and requirement for global information, decentralized control algorithms are deemed as a desirable alternative [17]. With advanced network

Manuscript received July 07, 2015; revised November 09, 2015; accepted December 04, 2015. Date of publication December 22, 2015; date of current version August 17, 2016. This work was supported by the Zhejiang Provincial Natural Science Foundation of China LR13F030002. Paper no. TPWRS-00965-2015.

H. Xing and Z. Lin are with the State Key Laboratory of Industrial Control Technology and the Department of Control Science and Engineering, Zhejiang University, Hangzhou 310027, China (e-mail: haoxing@zju.edu.cn; linz@zju.edu.cn).

M. Fu is with the School of Electrical Engineering and Computer Science, University of Newcastle, NSW 2308, Australia, and also with the State Key Laboratory of Industrial Control Technology and the Department of Control Science and Engineering, Zhejiang University, Hangzhou 310027, China (e-mail: minyue.fu@newcastle.edu.au).

Y. Mou is with the Center for Operations Research and Econometrics, Université catholique de Louvain, 1348 Louvain-la-Neuve, Belgium (e-mail: yuting.mou@uclouvain.be).

Color versions of one or more of the figures in this paper are available online at <http://ieeexplore.ieee.org>.

Digital Object Identifier 10.1109/TPWRS.2015.2507179

technologies, decentralized algorithms for control and optimization have been proposed by many researchers. Generally speaking, besides the feasibility and scalability in large-scale systems, the advantages of decentralized algorithms compared with centralized ones include reinforced robustness, reduction in communication and computation burden, and more balanced power consumption among agents [18].

Motivated by the overwhelming popularity of PEVs in the near future, this paper aims at the procurement of load shifting service during the night by utilizing both G2V and V2G of PEVs. Although existing works, e.g., [12], also propose decentralized scheduling strategies considering both G2V and V2G, to the best of the authors' knowledge, this is the first paper of which the objective is flattening the total demand curve as possible as it can be, in the configuration of bidirectional energy flow and decentralized algorithm. Our main contributions are summarized as follows:

- We formulate the optimal load shifting problem as an MDP problem, whose objective is to make the total demand curve as flat as possible while satisfying users' requirement of battery levels. Due to the NP-hardness of the primal MDP problem, we propose a reasonable and solvable problem approximation which fully exploits the shape feature of the typical base demand curve during the night. The basic idea of the problem approximation is to divide the whole time range into two periods with an optimal time threshold, before and after which the PEVs only charge and discharge, respectively.
- For the solvable approximated problem, we propose the decentralized optimal scheduling algorithm based on the iterative water-filling algorithm, which is decentralized in the sense that the PEVs conduct local computation and communicate with an aggregator. We also present detailed convergence analysis of the proposed algorithm.

The rest part of this paper is organized as follows. In Section II, a single PEV dynamic model, the problem formulation, and the decentralized water-filling based algorithm are presented. In Section III, we give an approximation of the primal optimization problem, and then propose a decentralized optimal scheduling algorithm. Simulation results are given in Section IV to show the performance of our algorithm. We conclude the paper in Section V.

II. PRELIMINARIES AND PROBLEM FORMULATION

In this section, we first introduce the dynamic model of a single PEV and the problem formulation, and then present the *decentralized water-filling-based algorithm* proposed in our previous work [7].

A. Dynamic Model of Single PEV

We assume that every PEV uses Lithium-ion batteries and has the capability of both G2V and V2G.

Let $t = 0, 1, \dots$ denote the time index with sampling interval ΔT . The SOC at time t , denoted by $s(t)(\%)$, is the charging level of a battery, which is given by

$$s(t) = \frac{C(t)}{C^{\max}}, \quad (1)$$

where C^{\max} (kWh) is the maximum capacity of the battery, and $C(t)$ (kWh) is the current amount of energy at time t .

Let $x(t)$ (kW) denote the power flow between the PEV and the grid. Assume that the PEV's charging or discharging rate is constant as $x(t)$ in the interval between t and $t + 1$. $x(t) > 0$ means that the PEV is charging at time t , while $x(t) < 0$ represents the discharging. $x(t) = 0$ if there is no power flow between the PEV and the grid.

We have the following inequality constraint:

$$-\bar{x}^{\text{out}} \leq x(t) \leq \bar{x}^{\text{in}}, \quad (2)$$

where \bar{x}^{in} is the maximum charging power, and \bar{x}^{out} is the maximum discharging power. For G2V, it is assumed that PEVs are outfitted with *smart chargers*, which can charge PEVs with any rate between 0 and \bar{x}^{in} . For V2G, PEVs are outfitted with *smart inverters*, which can discharge PEVs with any rate between 0 and \bar{x}^{out} .

Let us define $0 < \eta^{\text{in}}, \eta^{\text{out}} < 1$ as the energy conversion efficiencies of charging and discharging, respectively. Then the update of SOC follows

$$s(t+1) = s(t) + \eta(t)\Delta T \frac{x(t)}{C^{\max}}, \quad (3)$$

where ΔT is the aforementioned sampling interval and $\eta(t)$ is given by

$$\eta(t) = \begin{cases} \eta^{\text{in}} < 1, & \text{for } x(t) \geq 0, \\ \frac{1}{\eta^{\text{out}}} > 1, & \text{for } x(t) < 0. \end{cases}$$

To prolong the lifespan of the batteries, it is recommended that the SOC is kept in the range from 20% to 85% [19]. Suppose that the PEV will be unplugged at time T , and we have the following constraints.

$$\underline{s} \leq s(0) + \Delta T \frac{\sum_{t=0}^{\tau-1} \eta(t)x(t)}{C^{\max}} \leq \bar{s}, \quad \tau = 1, \dots, T, \quad (4)$$

where $s(0)$ is the initial SOC at time 0. In this paper we set $\underline{s} = 20\%$ and $\bar{s} = 85\%$.

The user of the PEV is able to set the desired SOC, denoted by s^* , which is the targeted SOC at time T . Note that $s^* \in [\underline{s}, \bar{s}]$. Then we have the following equality constraint,

$$s(0) + \Delta T \frac{\sum_{t=0}^{T-1} \eta(t)x(t)}{C^{\max}} = s^*. \quad (5)$$

B. Problem Formulation

In this paper we use PEVs with the capacity of both G2V and V2G to regulate the overall demand curve at night. For simplicity, we assume that the PEVs are plugged in at 20:00 and unplugged at 8:00 the next day. A typical overall demand (excluding PEVs) curve between 20:00 and 8:00 [20] is shown in Fig. 1.

The base load demand is denoted by $D(t)$, $\forall t = 0, \dots, T - 1$. Suppose that there are n PEVs, labelled from 1 to n . The parameters and variables are subscripted by $i = 1, \dots, n$, where i denotes the i th PEV. Denote the set made up of all the PEVs by V . The optimal load shifting problem is formulated as follows.

$$\min \sum_{t=0}^{T-1} \left(D(t) + \sum_{i=1}^n x_i(t) \right)^2. \quad (6)$$

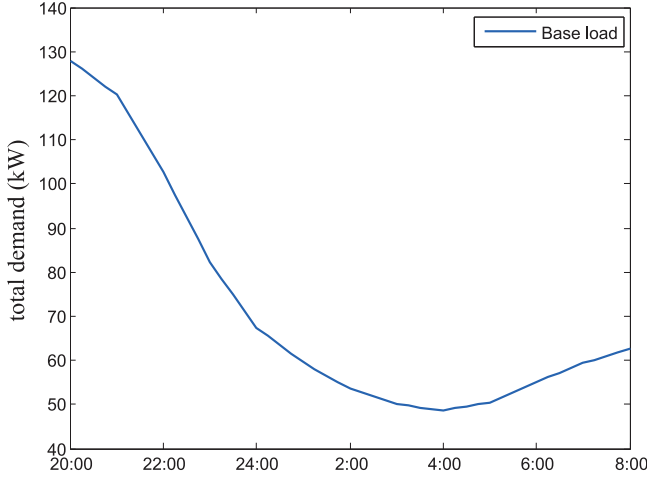


Fig. 1. Base load curve of 100 households in the service area of Southern California Edison from 20:00 on August 18, 2001 to 8:00 on August 19, 2011 [20].

- Constraints

- Equality constraints on $x_i(t)$'s

$$s_i(T) = s_i(0) + \Delta T \frac{\sum_{t=0}^{T-1} \eta_i(t) x_i(t)}{C_i^{\max}} = s_i^*, \quad \forall i. \quad (7)$$

- Inequality constraints on $x_i(t)$'s

$$-\bar{x}_i^{\text{out}} \leq x_i(t) \leq \bar{x}_i^{\text{in}}, \quad \forall i, t. \quad (8)$$

- Inequality constraints on $s_i(t)$'s

$$\underline{s} \leq s_i(t) \leq \bar{s}, \quad \forall i, t. \quad (9)$$

- Discrete constraints on $\eta_i(t)$'s

$$\eta_i(t) = \begin{cases} \eta_i^{\text{in}} < 1, & \text{for } x_i(t) \geq 0, \\ \frac{1}{\eta_i^{\text{out}}} > 1, & \text{for } x_i(t) < 0. \end{cases} \quad (10)$$

Remark 1: We note that in the optimization problem (6)–(10), the optimization variables include not only $x_i(t)$'s but also $\eta_i(t)$'s. Since $\eta_i(t)$'s can only take discrete values while $x_i(t)$'s take continuous values, the problem (6)–(10) is an MDP problem. And there are in total $3nT$ optimization variables. However, when only charging is considered, e.g., the work in [7], $\eta_i(t)$ is a constant equal to η_i^{in} , rather than a variable.

We want to achieve the optimal load shifting in a decentralized fashion with the assistance of an *aggregator*. The aggregator is assumed to know the forecast of the base load demand one day ahead. The communication topology between PEVs and the aggregator is a star network, where the aggregator is the central node, while the PEVs are the leaf nodes. The PEVs conduct bidirectional communication with the aggregator. The aggregator is not required to be computationally powerful, as the computational load will be evenly shared by each of the PEVs in our algorithm. Moreover, as we will show, the aggregator need not know the PEVs parameters, and therefore the users' privacy is kept.

C. Decentralized Water-Filling-Based Algorithm

Before proceeding to our decentralized scheduling algorithm, we now review the *decentralized water-filling-based algorithm* studied in our previous work [7].

Different from (2), the inequality constraints for PEVs used in [7] are given by

$$0 \leq x_i(t) \leq \bar{x}_i^{\text{in}}, \quad \forall i, t.$$

The users are also able to set their individual targeted SOCs, thus the equality constraints are the same as (5),

$$s_i(0) + \eta_i^{\text{in}} \Delta T \frac{\sum_{t=0}^{T-1} x_i(t)}{C_i^{\max}} = s_i^*, \quad \forall i.$$

The cost function is the same as (6), and then the integral problem formulation is given as follows.

$$\begin{aligned} \min \quad & \sum_{t=0}^{T-1} \left(D(t) + \sum_{i=1}^n x_i(t) \right)^2, \\ \text{s.t.} \quad & 0 \leq x_i(t) \leq \bar{x}_i^{\text{in}}, \quad \forall i, t, \\ & s_i(0) + \eta_i^{\text{in}} \Delta T \frac{\sum_{t=0}^{T-1} x_i(t)}{C_i^{\max}} = s_i^*, \quad \forall i. \end{aligned} \quad (11)$$

Define a projection mapping

$$\Gamma_i[r] = \begin{cases} \bar{x}_i^{\text{in}} & r > \bar{x}_i^{\text{in}}, \\ r & 0 \leq r \leq \bar{x}_i^{\text{in}}, \\ 0 & r < 0 \end{cases}. \quad (12)$$

Since in a smart grid scenario decentralized algorithms are preferred, we now recall the decentralized water-filling-based algorithm (Algorithm 1) which is proposed in [7].

Algorithm 1 Decentralized water-filling-based algorithm

Require: \bar{x}_i^{in} , ϵ , $s_i(0)$, s_i^* and $D(t)$, $\forall i, t$;

Ensure: $x_i(t)$, $\forall i, t$;

- 1: The aggregator gets the forecast of base load demand $D(t)$;
- 2: **for** $i = 1, 2, \dots, n$ **do**
- 3: The aggregator computes $D_i(t) = \sum_{j=1}^{i-1} x_j(t) + D(t)$, $\forall t, i \geq 2$; $D_i(t) = D(t)$, $\forall t, i = 1$;
- 4: The aggregator sends $D_i(t)$'s to the i th PEV;
- 5: For the i th PEV:
- 6: Initialize $\bar{\gamma}_i = \bar{x}_i^{\text{in}} + \max_t D_i(t)$ and $\underline{\gamma}_i = \min_t D_i(t)$;
- 7: **while** $\bar{\gamma}_i - \underline{\gamma}_i > \epsilon$ **do**
- 8: Compute $\gamma_i = (\bar{\gamma}_i + \underline{\gamma}_i)/2$;
- 9: Compute $x_i(t) = \Gamma_i[\gamma_i - D_i(t)]$ and $\sum_{t=0}^{T-1} x_i(t)$;
- 10: Update $\bar{\gamma}_i$ and $\underline{\gamma}_i$ following

$$\begin{cases} \bar{\gamma}_i = \gamma_i, \underline{\gamma}_i = \underline{\gamma}_i & \text{for } \eta_i^{\text{in}} \Delta T \frac{\sum_{t=0}^{T-1} x_i(t)}{C_i^{\max}} \geq s_i^* - s_i(0), \\ \bar{\gamma}_i = \bar{\gamma}_i, \underline{\gamma}_i = \gamma_i & \text{otherwise;} \end{cases}$$

11: **end while**

12: The i th PEV sends $x_i(t)$'s to the aggregator;

13: **end for**

The final water level, denoted by γ^* , actually satisfies that $\gamma^* = -\lambda^*$, where λ^* is the optimal *Lagrange multiplier*. The variable ϵ is defined as the tolerance of the gap between the upper and lower bounds of the water level, which is a very small positive number. Defining K as the number of bisection needed, we have

$$\epsilon \geq 2^K (\bar{\gamma} - \underline{\gamma}), \quad (13)$$

or

$$K \geq \log_2 \left(\frac{\bar{\gamma} - \underline{\gamma}}{\epsilon} \right). \quad (14)$$

From (14) we can see that a larger ϵ tends to cause a larger error to the final result but on the other hand it reduces the computational time. On the contrary, a smaller ϵ tends to increase the computational time while it also enhances the accuracy of the algorithm. Therefore the determination of ϵ depends on the specific need of different situations. When the algorithm's accuracy is more valued than its efficiency, a larger ϵ is chosen, and vice versa. See more details in [7].

Remark 2: In [7] we deal with the load management problem using only the charging of PEVs. The PEVs are outfitted with smart chargers and only able to achieve G2V. Therefore, in [7] only valley-filling (without peak shaving) is achieved. Algorithm 1 is termed as *water-filling* because the final result looks much like the natural phenomenon of water-filling, where $D(t)$ is the original water surface, while γ_n is the eventual water level after the water-filling.

III. MAIN RESULTS

In this section, we give an approximation of the primal optimization problem (6)–(10), propose a decentralized scheduling algorithm, and show the convergence analysis.

A. Problem Approximation

In this subsection we present an approximation of the primal problem (6)–(10). But before that, we first analyze the difficulty in directly solving the primal optimization problem (6)–(10):

- The optimization variables $x_i(t)$'s in the primal optimization problem (6)–(10) are strongly coupled, mainly due to the inequality constraints (9). The coexistence of charging and discharging forces us to take into consideration the constraints on SOCs. However, when only charging is considered, constraints (9) become redundant, making problem (11) easier to solve.
- The optimization variables $\eta_i(t)$'s in the primal optimization problem (6)–(10) takes discrete values. To appreciate the complexity that the discrete variables $\eta_i(t)$'s bring about, we comment that problem (6)–(10) can also be equivalently viewed as mixed integer nonlinear programming (MINLP) problem, which is NP-hard [21]. Furthermore, $\eta_i(t)$'s are dependent on $x_i(t)$'s, therefore they are also strongly coupled.

From the above discussion, we conclude that it is extremely hard to solve problem (6)–(10) directly, not to mention in a decentralized manner, which forces us to seek a reasonable and solvable approximation of problem (6)–(10).

Since we focus on flatten the total demand curve during the night, let us take a look back at Fig. 1. We can find the following shape feature of the base load curve:

- the peak load occurs at 20:00,
- the base demand decreases monotonically till around 4:00,
- and the base demand slightly increases from 4:00 to 8:00.

Other base load data from authoritative institutions, e.g., the hourly real-time system demand in New England ISO [22], real-time total load in Midwest ISO [23], have shown the same shape feature as that of Fig. 1. Therefore, it is reasonable to infer that, generally speaking, the overall base demand curve excluding PEVs during the night satisfies the following assumption:

Assumption 1: $D(t)$ is monotonically increasing in $[0, t_a]$, and reaches its maximum value at time t_a . Then in $[t_a, t_b]$, $D(t)$ is monotonically decreasing, and reaches its minimum value at time t_b . In $[t_b, T]$, $D(t)$ is monotonically increasing.

Note that in Fig. 1 that $t_a = 0$ and t_b is when the minimum demand is reached.

The ability of G2V enables the valley-filling, while V2G enables the peak shaving. That is to say, we can coordinate the PEVs such that the PEVs release power into the grid when the base load is at its peak, and charge when the base load is in the valley. In this way the overall demand curve is flattened. Since it is often the case that peak load occurs before the valley load, we want to find a time threshold t^\dagger , such that the PEVs discharge during $[0, t^\dagger]$ and charge during $[t^\dagger, T]$, and then find the optimal scheduling of PEVs' charging and discharging.

Divide set V into two subsets V_1 and V_2 , where $V_1 = \{i : s_i(0) > s^{\min}\}$, and $V_2 = \{i : s_i(0) \leq s^{\min}\}$. Based on the previous analysis, we give the following approximation of the primal problem (6)–(10).

$$\begin{aligned} \min \quad & \sum_{t=0}^{T-1} \left(D(t) + \sum_{i=1}^n x_i(t) \right)^2, \\ \text{s.t.} \quad & -\bar{x}_i^{\text{out}} \leq x_i(t) \leq 0, \forall t = 0, \dots, t^\dagger - 1, i \in V_1, \\ & x_i(t) = 0, \forall t = 0, \dots, t^\dagger - 1, i \in V_2, \\ & 0 \leq x_i(t) \leq \bar{x}_i^{\text{in}}, \forall t = t^\dagger, \dots, T - 1, i, \\ & s_i(0) + \Delta T \frac{\sum_{t=0}^{t^\dagger-1} \eta_i(t) x_i(t)}{C_i^{\max}} = s^{\min}, \forall i \in V_1, \\ & s_i(0) + \Delta T \frac{\sum_{t=0}^{T-1} \eta_i(t) x_i(t)}{C_i^{\max}} = s_i^*, \forall i, \end{aligned} \quad (15)$$

where t^\dagger , s^{\min} , $\eta_i(t)$'s, and $x_i(t)$'s are the optimization variables, and s^{\min} is defined as the targeted SOC at the end of the discharging stage, which is commonly shared by all the PEVs. Besides, for PEVs in subset V_2 , they do not discharge during $[0, t^\dagger]$, and they are only involved in the charging stage after t^\dagger .

Note that in problem (15), $\eta_i(t)$ is dependent on $x_i(t)$, and they are strongly coupled. If we fix certain t^\dagger and s^{\min} , we can further decompose problem (15) into the following two sub-problems, where $\eta_i(t)$'s are deterministic.

- For the discharging stage:

$$\begin{aligned} \min \quad & \sum_{t=0}^{t^\dagger-1} \left(D(t) + \sum_{i \in V_1} x_i(t) \right)^2, \\ \text{s.t.} \quad & -\bar{x}_i^{\text{out}} \leq x_i(t) \leq 0, \quad \forall t = 0, \dots, t^\dagger - 1, i \in V_1, \\ & s_i(0) + \frac{1}{\eta_i^{\text{out}}} \Delta T \frac{\sum_{t=0}^{t^\dagger-1} x_i(t)}{C_i^{\max}} = s^{\min}, \quad \forall i \in V_1. \end{aligned} \quad (16)$$

- For the charging stage:

$$\begin{aligned} \min \quad & \sum_{t=t^\dagger}^{T-1} \left(D(t) + \sum_{i=1}^n x_i(t) \right)^2, \\ \text{s.t.} \quad & 0 \leq x_i(t) \leq \bar{x}_i^{\text{in}}, \quad \forall t = t^\dagger, \dots, T-1, \\ & s^{\min} + \eta_i^{\text{in}} \Delta T \frac{\sum_{t=t^\dagger}^{T-1} x_i(t)}{C_i^{\max}} = s_i^*, \quad \forall i \in V_1, \\ & s_i(0) + \eta_i^{\text{in}} \Delta T \frac{\sum_{t=t^\dagger}^{T-1} x_i(t)}{C_i^{\max}} = s_i^*, \quad \forall i \in V_2. \end{aligned} \quad (17)$$

The optimization variables of problem (16) and (17) are only the $x_i(t)$'s. For fixed t^\dagger and s^{\min} , we can find the corresponding optimal solutions $x_i^*(t)$'s to problem (16) and (17), respectively. Problem (15) is therefore transformed into a bi-level programming problem (BLPP).

Remark 3: The cost function in (15) is the same as (6). The approximated problem differs from the primal optimization problem (6)–(10) in the constraints only. Inequality constraints (9) are absent in problem (15), making problem (15) easier to solve than problem (6)–(10).

B. Decentralized Optimal Scheduling Algorithm

Next we propose our decentralized optimal scheduling algorithm for the optimal load shifting problem using PEVs' charging and discharging, which is based on the decentralized water-filling-based algorithm. The core idea of our algorithm is to find t^\dagger and s^{\min} in a decentralized fashion, and then the $x_i(t)$'s are readily to get. The procedures are as follows, where for initialization we set $s^{\min} = \underline{s}$.

Step 1: All the PEVs use the decentralized water-filling-based algorithm to solve the following problem.

$$\begin{aligned} \min \quad & \sum_{t=0}^{T-1} \left(D(t) + \sum_{i=1}^n x_i(t) \right)^2, \\ \text{s.t.} \quad & 0 \leq x_i(t) \leq \bar{x}_i^{\text{in}}, \quad \forall t = 0, \dots, T-1, \\ & s^{\min} + \eta_i^{\text{in}} \Delta T \frac{\sum_{t=0}^{T-1} x_i(t)}{C_i^{\max}} = s_i^*, \quad \forall i \in V_1, \\ & s_i(0) + \eta_i^{\text{in}} \Delta T \frac{\sum_{t=0}^{T-1} x_i(t)}{C_i^{\max}} = s_i^*, \quad \forall i \in V_2. \end{aligned} \quad (18)$$

Denote the optimal solution to problem (18) by $x_i^{\text{in}}(t)$'s. After convergence, the aggregator will get a time point t^{in} such that

$$x_i^{\text{in}}(t) = 0, \quad \forall t < t^{\text{in}}, \text{ and } x_i^{\text{in}}(t^{\text{in}}) > 0, \quad \forall i. \quad (19)$$

There is a corresponding water level, denoted by γ^{in} , which follows

$$\gamma^{\text{in}} = D(t^{\text{in}}) + \sum_{i=1}^n x_i(t^{\text{in}}).$$

Step 2: Since only PEVs in subset V_1 will be involved in the discharging stage, let the PEVs in subset V_1 use the de-

centralized water-filling-based algorithm to solve the following problem:

$$\begin{aligned} \min \quad & \sum_{t=0}^{T-1} \left(D(t) + \sum_{i \in V_1} x_i(t) \right)^2, \\ \text{s.t.} \quad & -\bar{x}_i^{\text{out}} \leq x_i(t) \leq 0, \quad \forall t = 0, \dots, T-1, i \in V_1, \\ & s_i(0) + \frac{1}{\eta_i^{\text{out}}} \Delta T \frac{\sum_{t=0}^{T-1} x_i(t)}{C_i^{\max}} = s^{\min}, \quad \forall i \in V_1, \end{aligned} \quad (20)$$

where we set $s^{\min} = \underline{s}$. Denote the optimal solution to problem (20) by $x_i^{\text{out}}(t)$'s. For PEVs in V_2 , set $x_i^{\text{out}} = 0, \forall t$. After convergence, the aggregator will get a time point t^{out} such that

$$x_i^{\text{out}}(t) = 0, \quad \forall t > t^{\text{out}}, \text{ and } x_i^{\text{out}}(t^{\text{out}}) < 0, \quad \forall i \in V_1. \quad (21)$$

Though in this step we use the water-filling-based algorithm, but the outcome looks like *peaking shaving*, or *inverse water-filling*. The corresponding water level, denoted by γ^{out} , follows

$$\gamma^{\text{out}} = D(t^{\text{out}}) + \sum_{i \in V_1} x_i(t^{\text{out}}).$$

Step 3: In this step, the aggregator compares the two water levels. With Assumption 1 satisfied, t^{out} and t^{in} shall fall into the interval $[t_a, t_b]$. Due to the decreasing monotonicity, judging whether $\gamma^{\text{out}} \geq \gamma^{\text{in}}$ is equivalent to judging if $t^{\text{out}} \leq t^{\text{in}}$.

- If $t^{\text{out}} \leq t^{\text{in}}$ holds, then the optimal solution to problem (15) is that

$$t^\dagger \in [t^{\text{out}}, t^{\text{in}}], \quad s^{\min} = \underline{s},$$

and

$$x_i^*(t) = x_i^{\text{out}}(t) + x_i^{\text{in}}(t), \quad \forall t, i.$$

- Otherwise, the aggregator establishes a new auxiliary variable $\alpha = (\underline{s} + \bar{s})/2$, and the algorithm returns to Step 1 by setting $s^{\min} = \alpha$.

After achieving Step 1 and 2, by comparing the new γ^{out} and γ^{in} , the aggregator updates \underline{s} , \bar{s} , and α using

$$\begin{cases} \bar{s} = \alpha, \underline{s} = \underline{s} & \text{if } \gamma^{\text{out}} > \gamma^{\text{in}}, \\ \underline{s} = \alpha, \bar{s} = \bar{s} & \text{if } \gamma^{\text{out}} < \gamma^{\text{in}}, \end{cases}$$

and

$$\alpha = (\underline{s} + \bar{s})/2.$$

Rerun this step until $\gamma^{\text{out}} = \gamma^{\text{in}}$. Then the optimal solution to problem (15) is that

$$t^\dagger = t^{\text{in}} = t^{\text{out}}, \quad s^{\min} = s^*,$$

and

$$x_i^*(t) = x_i^{\text{out}}(t) + x_i^{\text{in}}(t), \quad \forall t, i.$$

The following are some interpretations about the proposed algorithm:

- Theoretically, there are possibilities that we cannot find t^{in} or t^{out} such that (21) or (19) holds, respectively. Let us take t^{out} for example. There are in total two situations where t^{out} does not exist: 1) The discharging of PEVs shaves the entire curve off, including the valley part, i.e., $\min_t (D(t) + \sum_{i \in V_1} x_i^{\text{out}}) < \min_t D(t)$. 2) There may exist $t^{\text{in}'} > t^{\text{in}}$ such that the PEVs discharge during the in-

terval $[t^{\text{in}}, t^{\text{in}'}]$. However, both situations are ruled out in practice. Firstly, the PEVs do not have such large residual energy such that their discharging could shave the whole curve off. Secondly, the practical disparity between the peak and the valley is sufficiently large to make sure situation 2) will not happen, either.

- The ideal regulated total demand curve shall be a straight line, which usually does not hold in practice due to limited rate of charging and discharging, and finite penetration rate of PEVs. But with optimal scheduling of charging and discharging, it is impossible that the regulated water level in the discharging stage is lower than that of the charging stage, i.e., $\gamma^{\text{out}} \geq \gamma^{\text{in}}$ must hold.
- In Step 3, if $t^{\text{out}} > t^{\text{in}}$, we can infer that the PEVs release too much energy back to the grid. So in this case we have to increase s^{min} such that $\gamma^{\text{out}} = \gamma^{\text{in}}$. We obtain s^{min} by adopting the idea of *bisection* in a decentralized fashion.

Remark 4: The algorithm proposed in this paper is based on the water-filling-based algorithm in our previous work [7], and it is easily verified that our algorithm is also decentralized. Moreover, the decentralization of our algorithm on one hand reduces the computational burden of the aggregator, and on the other hand, keeps the users' privacy. The aggregator does not need to know any of the PEVs' parameters.

Remark 5: To satisfy the Assumption 1, it may implicitly require a large population of loads, such that the aggregated behavior of all the households follows a certain pattern, while the unexpected behavior of a single household has little influence on the aggregated behavior. We therefore believe that the Assumption 1 may not be satisfied for small load populations. For example, the night demand curve of a micro-grid may have multiple peaks and valleys. To deal with this situation, the demand curve can be divided into multiple sub-curves, where each sub-curve satisfies the Assumption 1. Then at the end of each sub-curve, phased target SOC's are assigned such that the assignment is optimal and the phased target SOC of the last sub-curve equals the target SOC of the whole curve. Then the proposed algorithm can be applied to each sub-curve to get the solution regarding the whole curve.

C. Convergence Analysis

Next we give a result about the convergence of our decentralized optimal scheduling algorithm.

Theorem 1: If there exist t^{out} and t^{in} such that conditions (21) and (19) hold and $t^{\text{out}} \leq t^{\text{in}}$, then the proposed algorithm converges to the optimal solution to problem (15).

For the proof of Theorem 1, the following lemmas are needed. Lemma 1 is about the optimal water-filling using one single PEV.

Lemma 1 [7]: The optimal solution to problem

$$\begin{aligned} \min \quad & \sum_{t=0}^{T-1} (D(t) + x(t) - \omega)^2, \\ \text{s.t.} \quad & 0 \leq x(t) \leq \bar{x}^{\text{in}}, \quad \forall t, \\ & s(0) + \eta^{\text{in}} \Delta T \frac{\sum_{t=0}^{T-1} x(t)}{C^{\text{max}}} = s^* \end{aligned} \quad (22)$$

is given by

$$x^*(t) = \Gamma[-\lambda^* - D(t)], \quad \forall t,$$

where ω is the *ideal aggregate demand*, which is constant for all t , $x^*(t)$ is the optimal solution to problem (22), λ^* is the optimal *Lagrange multiplier*, and $\Gamma[\cdot]$ is given by (12).

Lemma 2: The optimal solution to problem (22) is not subject to the ideal demand ω .

Proof: We have

$$\begin{aligned} \sum_{t=0}^{T-1} (D(t) + x(t) - \omega)^2 &= \sum_{t=0}^{T-1} (D(t) + x(t))^2 \\ &\quad + 2\omega \sum_{t=0}^{T-1} x(t) + T\omega^2. \end{aligned} \quad (23)$$

According to the equality constraint on $x(t)$'s, it follows that

$$\sum_{t=0}^{T-1} x(t) = (s^* - s(0))C^{\text{max}}/(\eta^{\text{in}} \Delta T), \quad (24)$$

which is a constant. Therefore, combining (23) and (24), we have

$$\sum_{t=0}^{T-1} (D(t) + x(t) - \omega)^2 = \sum_{t=0}^{T-1} (D(t) + x(t))^2 + \rho(\omega),$$

where

$$\rho(\omega) = 2\omega(s^* - s(0))C^{\text{max}}/(\eta^{\text{in}} \Delta T) + T\omega^2.$$

Therefore ω only controls the constant term of the cost function, and Lemma 2 is proved. \blacksquare

Now we give the proof of Theorem 1.

Proof of Theorem 1: We first define

$$\begin{aligned} c_t(x(t), \omega) &= \left(D(t) + \sum_{i=1}^n x_i(t) - \omega \right)^2, \\ C(x, \omega) &= \sum_{t=0}^{T-1} c_t(x, \omega). \end{aligned}$$

It follows that the cost (6) is equal to $C(x, 0)$.

After the proposed algorithm converges, there will be 2 kinds of outcomes:

A: We first prove that t^\dagger is optimal by contradiction. Let us say, there is such $t^\ddagger < t^{\text{out}}$ that t^\ddagger makes the total cost lower than t^\dagger does. Denote by $x_i^\ddagger(t)$ the optimal solution with t^\ddagger . According to Lemma 2, we replace the initial cost function by $C(x, \gamma^{\text{out}})$ without making any changes to the optimal solution. The whole charging and discharging process can be divided into three parts accordingly:

- For $t \in [0, t^\ddagger]$, we deal with problem (16) using Algorithm 1 with t^\dagger replaced by t^\ddagger . Denote the corresponding eventual water level by $\gamma^{\ddagger \text{out}}$. According to the nature of inverse water-filling, $t^\ddagger < t^\dagger$ leads to $\gamma^{\ddagger \text{out}} < \gamma^{\text{out}}$. Since

we shrink the discharging time and the problem is still feasible, from Lemma 1, there must exist some t such that $x_i^*(t) > -\bar{x}_i^{\text{out}}$. Therefore we have

$$\begin{cases} x_i^\dagger(t) = -\bar{x}_i^{\text{out}}, & \text{if } x_i^*(t) = -\bar{x}_i^{\text{out}}, \\ x_i^\dagger(t) < x_i^*(t), & \text{if } x_i^*(t) > -\bar{x}_i^{\text{out}}. \end{cases}$$

It leads to that for $t \in [0, t^\dagger]$,

$$D(t) + \sum_{i=1}^n x_i^\dagger(t) \leq D(t) + \sum_{i=1}^n x_i^*(t),$$

where the equality holds only at t when $x_i^*(t) = -\bar{x}_i^{\text{out}}$. Furthermore, we know that there exists some time t such that

$$\begin{aligned} D(t) + \sum_{i=1}^n x_i^*(t) - \gamma^{\text{out}} &= 0, \\ D(t) + \sum_{i=1}^n x_i^\dagger(t) - \gamma^{\text{out}} &< 0. \end{aligned}$$

Therefore we have

$$\sum_{t=0}^{t^\dagger-1} c_t(x^\dagger(t), \gamma^{\text{out}}) > \sum_{t=0}^{t^\dagger-1} c_t(x^*, \gamma^{\text{out}}). \quad (25)$$

- For $t \in [t^\dagger, t^{\text{in}}]$, we have $-\bar{x}_i^{\text{out}} \leq x_i^*(t) < 0$ and $x_i^\dagger(t) = 0$. Since $D(t) + \sum_{i=1}^n x_i^*(t) = \gamma^{\text{out}}$, it follows that

$$\sum_{t^\dagger}^{t^{\text{in}}-1} c_t(x^\dagger(t), \gamma^{\text{out}}) > \sum_{t^\dagger}^{t^{\text{in}}-1} c_t(x^*, \gamma^{\text{out}}). \quad (26)$$

- For $t > t^{\text{in}}$, since $t^\dagger < t^{\text{in}}$, according to Lemma 1 we have $x_i^\dagger(t) = x_i^*(t)$. It follows that

$$\sum_{t=t^{\text{in}}}^{T-1} c_t(x^\dagger(t), \gamma^{\text{out}}) = \sum_{t=t^{\text{in}}}^{T-1} c_t(x^*, \gamma^{\text{out}}). \quad (27)$$

From (25)–(27), we have

$$C(x^\dagger, \gamma^{\text{out}}) > C(x^*, \gamma^{\text{out}}),$$

which contradicts the assumption. Similarly we can conclude that there is no $t^\dagger > t^{\text{in}}$ such that the total cost is further lowered. So t^\dagger is optimal.

B: We next prove in this scenario s^{min} is optimal by contradiction as well. Let us say, there exists $s^\diamond > s^{\text{min}}$ such that the total cost is further lowered. Denote by $x_i^\diamond(t)$ the optimal solution with s^\diamond . We still use the cost function $C(x, \gamma^{\text{out}})$ in this case.

The adoption of s^\diamond leads to a new set of demarcation points, denoted by $t^{\diamond, \text{out}}$ and $t^{\diamond, \text{in}}$, respectively. There are also two new water levels accordingly, denoted by $\gamma^{\diamond, \text{out}}$ and $\gamma^{\diamond, \text{in}}$. In this case, the PEVs release less power into the grid. Due to the nature of water-filling, one can easily verify that

$$\begin{aligned} t^{\diamond, \text{out}} < t^{\text{out}} < t^{\text{in}} < t^{\diamond, \text{in}}, \\ \gamma^{\diamond, \text{out}} > \gamma^{\text{out}} > \gamma^{\text{in}} > \gamma^{\diamond, \text{in}}. \end{aligned}$$

In words, the new water levels $\gamma^{\diamond, \text{out}}$ and $\gamma^{\diamond, \text{in}}$ both move further away from γ^{out} . Applying the same techniques used in Case A, we have the following statements

$$\begin{cases} \sum_{t=0}^{t^{\diamond, \text{out}}-1} c_t(x^\diamond(t), \gamma^{\text{out}}) > \sum_{t=0}^{t^{\diamond, \text{out}}-1} c_t(x^*, \gamma^{\text{out}}), \\ \sum_{t=t^{\diamond, \text{out}}}^{t^{\text{in}}-1} c_t(x^\diamond(t), \gamma^{\text{out}}) = \sum_{t=t^{\diamond, \text{out}}}^{t^{\text{in}}-1} c_t(x^*, \gamma^{\text{out}}), \\ \sum_{t=t^{\text{in}}}^{T-1} c_t(x^\diamond(t), \gamma^{\text{out}}) > \sum_{t=t^{\text{in}}}^{T-1} c_t(x^*, \gamma^{\text{out}}). \end{cases} \quad (28)$$

From (28), we have

$$C(x^\diamond, \gamma^{\text{out}}) > C(x^*, \gamma^{\text{out}}),$$

which contradicts the assumption. Similarly we can conclude that there is no $s^\diamond < s^{\text{min}}$ such that the total cost is further lowered. So s^{min} is optimal. ■

IV. NUMERICAL SIMULATIONS

In this section we give some simulation results to show how our algorithm works. We first use only 5 homogenous PEVs to regulate the total demand of 100 households, and then we apply the proposed algorithm to 10 heterogenous PEVs. At last we make comparisons between the proposed algorithm and the existing approach to further show the effectiveness of our algorithm.

A. Case 1: Dealing With 5 Homogenous PEVs

In this case, we use only 5 homogenous PEVs for the optimal load shifting of 100 households. The base load demand of the 100 households is shown in Fig. 1. We assume that all the PEVs join in the grid at 20:00, and leave at 8:00 the next day. The PEVs' parameters are as follows: $\bar{x}_i^{\text{in}} = 4$ kW, $\bar{x}_i^{\text{out}} = 4$ kW, $C_i^{\text{max}} = 25$ kWh, $\underline{s} = 20\%$, $\bar{s} = 85\%$, $\eta^{\text{in}} = 95\%$, $(1)/(\eta^{\text{out}}) = 110\%$, and $s_i^* = 85\%$. We set the sampling period $\Delta T = 15$ min. The PEVs initial SOC are heterogenous, given by $s_1(0) = 33.1148\%$, $s_2(0) = 20.7142\%$, $s_3(0) = 36.9826\%$, $s_4(0) = 38.6799\%$, and $s_5(0) = 33.5747\%$.

We set $s^{\text{min}} = \underline{s} = 20\%$. The results of step 1 and 2 are shown in Fig. 2. We can see that after performing the first 2 steps, the water level of the discharging process is higher than that of the charging process, i.e., $\gamma^{\text{out}} > \gamma^{\text{in}}$. Then according to step 3, there is no need to reselect s^{min} , and we can have the optimal scheduling of charging and discharging, as it is shown in Fig. 3.

We also compare the peaking load shifting using both charging and discharging of PEVs with optimal valley filling (Algorithm 1) using only the charging process. One can easily verify that besides the ‘‘inverse water filling’’ from 20:00 to 21:30, the water level of our algorithm in the charging stage is higher than that of Algorithm 1. Therefore, we can infer that the curve is more flattened using both the charging and discharging of PEVs.

B. Case 2: Dealing With 10 Heterogenous PEVs

In this case, we deal with PEVs with a higher penetration rate. Different from Case 1, 10 heterogenous PEVs are used in this

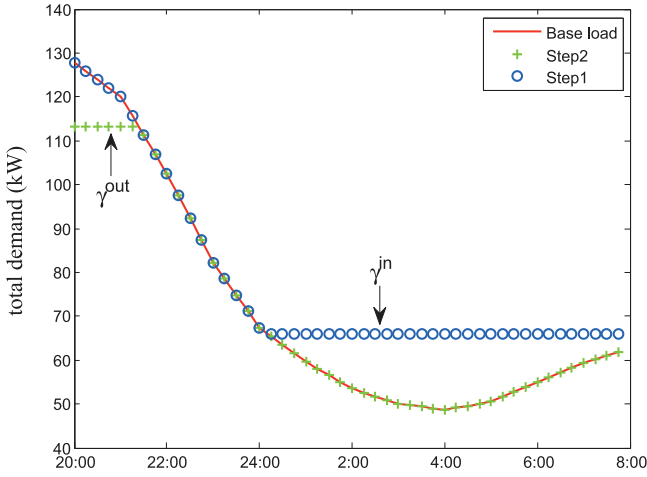


Fig. 2. The results of step 1 and step 2, dealing with 5 PEVs.

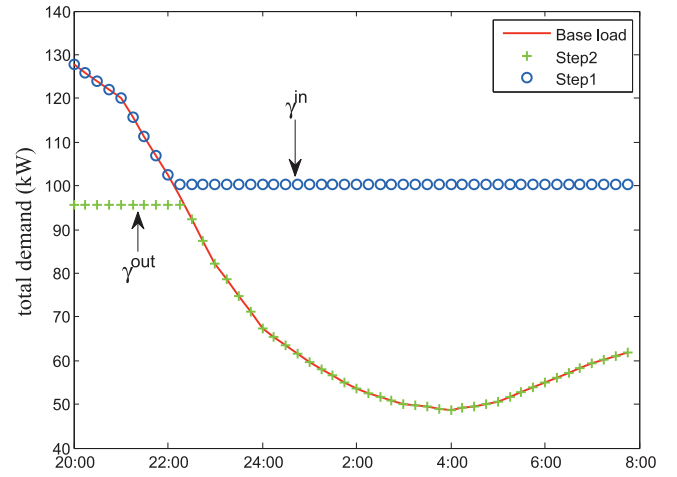


Fig. 4. The results of step 1 and step 2, dealing with 10 PEVs.

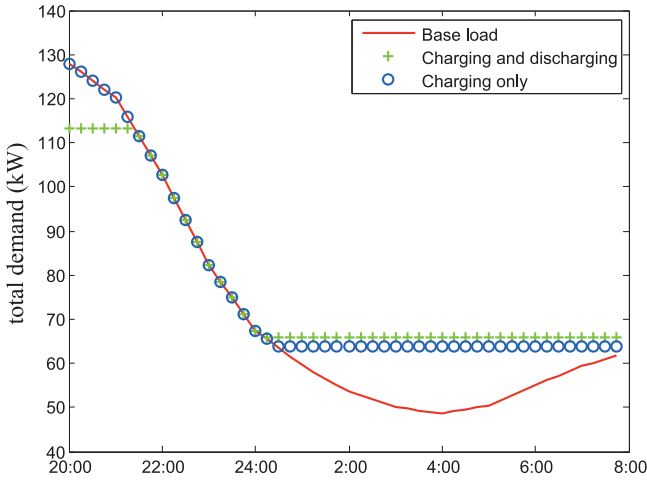


Fig. 3. Optimal load shifting using charging and discharging.

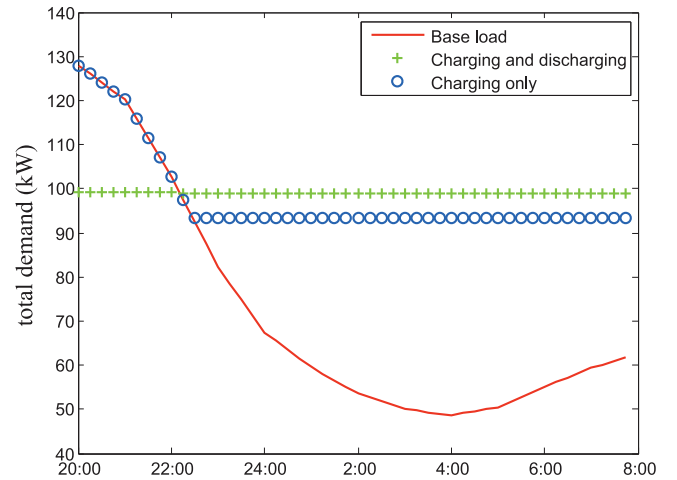


Fig. 5. Optimal load shifting using charging and discharging.

case. The homogenous parameters are given as follows, and the unlisted parameters are the same as those in Case 1.

$$\begin{aligned} \bar{x}^{\text{in}} = \bar{x}^{\text{out}} (\text{kW}) &= 6.8064 \ 9.3228 \ 8.4236 \ 6.7122 \ 7.2912 \\ &\quad 8.1500 \ 9.4640 \ 9.4876 \ 6.9044 \ 9.5058, \\ s(0) (\%) &= 33.114 \ 20.714 \ 36.982 \ 38.679 \ 33.574 \\ &\quad 35.154 \ 34.862 \ 27.844 \ 33.109 \ 23.423, \\ C^{\text{max}} (\text{kWh}) &= 42.539 \ 58.267 \ 52.647 \ 41.950 \ 45.570 \\ &\quad 50.937 \ 59.150 \ 59.297 \ 43.152 \ 59.411, \\ \eta^{\text{in}} (\%) &= 95.530 \ 90.340 \ 93.800 \ 86.560 \ 89.640 \\ &\quad 95.070 \ 93.710 \ 95.550 \ 92.210 \ 85.390, \\ \frac{1}{\eta^{\text{out}}} (\%) &= 112.85 \ 108.82 \ 110.01 \ 115.57 \ 107.93 \\ &\quad 111.77 \ 116.62 \ 109.18 \ 108.34 \ 108.53. \end{aligned}$$

We first set $s^{\text{min}} = \underline{s} = 20\%$. The results of step 1 and 2 are shown in Fig. 4. We can see that after performing the first 2 steps, the water level of the discharging process is lower than that of the discharging process, i.e., $\gamma^{\text{out}} < \gamma^{\text{in}}$. That means the PEVs do not need to release that much power back into the grid, so we need to find the optimal s^{min} using step 3 adopting the idea of bisection. The final result is shown in Fig. 5, where

the optimal s^{min} turns out to be 22.03%. We can see that our decentralized optimal scheduling algorithm does not only apply to homogenous population of PEVs, but also heterogeneous ones. In this case, the regulated total demand curve turns into a straight line, and one can see that the optimal load shifting using both charging and discharging is much better than merely the valley filling using the charging process only.

C. Case 3: Comparisons Between Proposed Algorithm and BONMIN

In this case we make comparisons between the proposed algorithm and the existing mixed integer programming approach. Since the original problem (6)–(10) can be viewed as a MINLP problem, we use the basic open-source nonlinear mixed integer programming (BONMIN) which is a powerful solver for general MINLP problems, to solve the original problem [24]. Specifically, an hybrid outer-approximation based branch-and-cut algorithm (also referred to as B-Hyb) is chosen in the implementation of BONMIN. See [25] for more details about the B-Hyb algorithm.

The proposed algorithm and the BONMIN solver are tested with various amount of homogenous PEVs from 1 to 10. We assume that all the PEVs join in the grid at 20:00, and leave at

TABLE I
COMPUTATIONAL TIME OF THE PROPOSED ALGORITHM AND BONMIN
APPLIED TO VARIOUS NUMBERS OF PEVS

Time (sec) Number	Algorithm	
	Our algorithm	BONMIN
1	0.00988	38.61
2	0.01097	203.99
3	0.01126	158.93
4	0.01137	1651.57
5	0.01204	4378.32
10	0.01240	93492.93

8:00 the next day, like in the first two cases. The parameters of the PEVs are adapted from Case 1.

To rule out uncertainty factors, both of the two algorithms are tested in the MATLAB environment on the author's laptop with Intel Core i7-3610QM processor and 8 GB DDR3 memory. Both of the two algorithms successfully converge to the optimal solutions, but their computational speeds are quite different. The computational time of the proposed algorithm and BONMIN applied to various amounts of PEVs is presented in Table I.

One can easily verify that the computational speed of our algorithm is much faster than that of BONMIN. The computational time taken by our algorithm is on a microsecond basis, and it just slightly increases as the number of PEVs rises. Nevertheless, the computational time taken by BONMIN increases significantly with the number of PEVs. It even takes 93492.93 seconds, which approximate 26 hours, to solve the optimal charging and discharging scheduling of only 10 PEVs, which it takes only 12.4 microseconds by our algorithm. Since in practice we are usually faced with hundreds or even thousands of PEVs, we can conclude that BONMIM is almost unapplicable to this optimal scheduling problem.

V. CONCLUDING REMARKS

In this paper, we have investigated the problem of using PEVs' charging and discharging for optimal load shifting. We first formulate the problem as an MDP problem, which is extremely hard to solve directly. Exploiting the shape feature of the base load curve during the night, we present a solvable approximation of the primal problem, for which a decentralized optimal scheduling algorithm is proposed. Using our algorithm, all the PEVs are charged to the targeted SOC's and the total demand curve is flattened. Our algorithm is decentralized in the sense that the PEVs compute locally and communicate with an aggregator. Future work would be dealing with demand curves of general shapes which do not necessarily satisfy the Assumption 1. Dynamic networks of PEVs, where PEVs can join and leave from time to time, and the existence of flexible loads and renewable energy sources will also be considered in the future.

REFERENCES

[1] J. A. P. Lopes, F. J. Soares, and P. M. R. Almeida, "Integration of electric vehicles in the electric power system," *Proc. IEEE*, vol. 99, no. 1, pp. 168–183, Jan. 2011.

[2] B. K. Sovacool and R. F. Hirsh, "Beyond batteries: An examination of the benefits and barriers to plug-in hybrid electric vehicles (PHEVs) and a vehicle-to-grid (v2g) transition," *Energy Policy*, vol. 37, no. 3, pp. 1095–1103, 2009.

[3] K. Clement-Nyns, E. Haesen, and J. Driesen, "The impact of charging plug-in hybrid electric vehicles on a residential distribution grid," *IEEE Trans. Power Syst.*, vol. 25, no. 1, pp. 371–380, Feb. 2010.

[4] V. C. Güngör, D. Sahin, T. Kocak, S. Ergüt, C. Buccella, C. Cecati, and G. P. Hancke, "Smart grid technologies: Communication technologies and standards," *IEEE Trans. Ind. Informat.*, vol. 7, no. 4, pp. 529–539, 2011.

[5] Z. Ma, D. Callaway, and I. Hiskens, "Decentralized charging control for large populations of plug-in electric vehicles," in *Proc. 49th IEEE Conf. Decision and Control*, 2010, pp. 206–212.

[6] L. Gan, U. Topcu, and S. Low, "Optimal decentralized protocol for electric vehicle charging," *IEEE Trans. Power Syst.*, vol. 28, no. 2, pp. 940–951, May 2013.

[7] Y. Mou, H. Xing, Z. Lin, and M. Fu, "A new approach to distributed charging control for plug-in hybrid electric vehicles," in *Proc. 33rd Chinese Control Conf.*, 2014.

[8] Y. Mou, H. Xing, Z. Lin, and M. Fu, "Decentralized optimal demand-side management for PHEV charging in a smart grid," *IEEE Trans. Smart Grid*, accepted for publication.

[9] Y. Mou, H. Xing, M. Fu, and Z. Lin, "Decentralized PWM based charging control for plug-in electric vehicles," in *Proc. European Control Conf. (ECC)*, 2015.

[10] C. Goebel and D. Callaway, "Using ICT-controlled plug-in electric vehicles to supply grid regulation in California at different renewable integration levels," *IEEE Trans. Smart Grid*, vol. 4, no. 2, pp. 729–740, 2013.

[11] C. Guille and G. Gross, "A conceptual framework for the vehicle-to-grid (V2G) implementation," *Energy Policy*, vol. 37, no. 11, pp. 4379–4390, 2009.

[12] Y. He, B. Venkatesh, and L. Guan, "Optimal scheduling for charging and discharging of electric vehicles," *IEEE Trans. Smart Grid*, vol. 3, no. 3, pp. 1095–1105, 2012.

[13] A. Y. Saber and G. K. Venayagamoorthy, "Resource scheduling under uncertainty in a smart grid with renewables and plug-in vehicles," *IEEE Syst. J.*, vol. 6, no. 1, pp. 103–109, 2012.

[14] M. E. Khodayar, L. Wu, and M. Shahidehpour, "Hourly coordination of electric vehicle operation and volatile wind power generation in SCUC," *IEEE Trans. Smart Grid*, vol. 3, no. 3, pp. 1271–1279, 2012.

[15] L. Jian, H. Xue, G. Xu, X. Zhu, D. Zhao, and Z. Shao, "Regulated charging of plug-in hybrid electric vehicles for minimizing load variance in household smart microgrid," *IEEE Trans. Ind. Electron.*, vol. 60, no. 8, pp. 3218–3226, 2013.

[16] M. Tushar, C. Assi, M. Maier, and M. Uddin, "Smart microgrids: Optimal joint scheduling for electric vehicles and home appliances," *IEEE Trans. Smart Grid*, vol. 5, no. 1, pp. 239–250, 2014.

[17] L. Bakule, "Decentralized control: An overview," *Ann. Rev. Control*, vol. 32, no. 1, pp. 87–98, 2008.

[18] Z. Lin, *Distributed Control and Analysis of Coupled Cell Systems*. Saarbrücken, Germany: VDM Publishing, 2008.

[19] Q. Wu, A. H. Nielsen, J. Østergaard, S.-T. Cha, F. Marra, and P. B. Andersen, "Modeling of electric vehicles (evs) for ev grid integration study," in *Proc. 2nd Eur. Conf. Smart Grids & E-Mobility*, Brussels, Belgium, 2010.

[20] South California Edison [Online]. Available: https://www.sce.com/005_regul_info/eca/DOMSM11.DLP

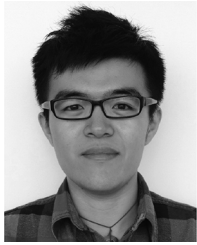
[21] H. W. Lenstra, Jr, "Integer programming with a fixed number of variables," *Math. Oper. Res.*, vol. 8, no. 4, pp. 538–548, 1983.

[22] Hourly Real-Time System Demand in New England ISO [Online]. Available: <http://www.iso-ne.com/isoexpress/web/reports/load-and-demand/-/tree/dmnd-rt-hourly-sys>

[23] Real-Time Total Load in Midwest ISO [Online]. Available: <https://www.misoenergy.org/MarketsOperations/RealTimeMarket-Data/Pages/RealTimeTotalLoad.aspx> [Online]. Available:

[24] Basic Open-Source Nonlinear Mixed Integer Programming [Online]. Available: <http://www.coin-or.org/Bonmin/>

[25] P. Bonami *et al.*, "An algorithmic framework for convex mixed integer nonlinear programs," *Discrete Optimiz.*, vol. 5, no. 2, pp. 186–204, 2008.



Hao Xing (S'14) received his Bachelor degree from Zhejiang University, China, in 2012. He is currently working towards a Ph.D. degree in the Department of Control Science and Engineering, Zhejiang University, China. He is also a visiting scholar at the Department of Geography and Environmental Engineering, The Johns Hopkins University.

His research interests focus on distributed algorithms for control and optimization in smart grid.



Minyue Fu (F'03) received his Bachelors degree from the University of Science and Technology of China in 1982, and M.S. and Ph.D. degrees from the University of Wisconsin-Madison in 1983 and 1987, respectively.

From 1987 to 1989, he was an Assistant Professor at Wayne State University, USA. He joined University of Newcastle, Australia, in 1989 and was promoted to a Chair Professor in 2002. He has served as the Head of Department and Head of School for over 7 years. He has been a Visiting Professor at Uni-

versity of Iowa, Nanyang Technological University and Tokyo University. He has held a Changjiang Visiting Professorship at Shandong University and a Qian-ren Professorship at Zhejiang University. His main research interests include control systems, signal processing and communications. His current research projects include networked control systems, smart electricity networks. He has published nearly 350 papers, including 120 or so journal papers.

Dr. Fu has been an Associate Editor for the IEEE TRANSACTIONS ON AUTOMATIC CONTROL, IEEE TRANSACTIONS ON SIGNAL PROCESSING, *Automatica* and *Journal of Optimization and Engineering*.



Zhiyun Lin (SM'10) received his Bachelor degree in electrical engineering from Yanshan University, China, in 1998, Master degree in electrical engineering from Zhejiang University, China, in 2001, and Ph.D. degree in electrical and computer engineering from the University of Toronto, Canada, 2005. He was a Postdoctoral Research Associate in the Department of Electrical and Computer Engineering, University of Toronto, Canada, from 2005 to 2007.

He joined the College of Electrical Engineering, Zhejiang University, China, in 2007. Currently, he is a Professor of Systems Control in the same department. He is also affiliated with the State Key Laboratory of Industrial Control Technology at Zhejiang University. He held visiting professor positions at several universities including The Australian National University (Australia), University of Cagliari (Italy), University of Newcastle (Australia), and University of Technology Sydney (Australia). His research interests focus on distributed control, estimation and optimization, coordinated and cooperative control of multi-agent systems, hybrid and switched system theory, and locomotion control of biped robots.

Dr. Lin is currently an associate editor for *Hybrid Systems: Nonlinear Analysis* and *International Journal of Wireless and Mobile Networking*.



Yuting Mou received the Bachelors and Masters degrees in electrical engineering from Jilin University, Changchun, China, and Zhejiang University, Hangzhou, China, in 2012 and 2015, respectively. He is currently a Ph.D. student in power system operation and economics at Université catholique de Louvain, Belgium.

His research interests include demand response in smart grid and distributed optimization.